



Original

## One Dimensional Modeling of Jet Diffusion Flame

Angan Sengupta <sup>a,\*</sup>, A.K. Gupta <sup>b</sup>, I.M. Mishra <sup>c</sup>, S. Suresh <sup>d</sup>

<sup>a</sup> Department of Chemical Engineering, Birla Institute of Technology & Science, Pilani, Hyderabad Campus, Hyderabad 500078, Telengana, India.

<sup>b</sup> Scientist and former Head, Fire Research Laboratory, Central Building Research Institute, Roorkee, India.

<sup>c</sup> Department of Chemical Engineering, Department of Chemical Engineering Indian school of Mines, Dhanbad-826004, Jharkhand, India.

<sup>d</sup> Advanced Analytical and Simulation Research Laboratory, Department of Chemical Engineering, National Institute of Technology, Bhopal, Bhopal 462 003, M.P., India.

---

**Abstract:** This paper reports on the determination of the flame height of a flare system using theoretical approach based on the laws of conservation of mass, momentum and energy. The set of ordinary differential equations at steady state conditions are solved numerically by fourth order Runge–Kutta method. The extent of reaction between the fuel and the entrained air has been studied by introducing the reaction mixing efficiency parameter, as the reaction rate is fixed by local entrainment rate. The reaction mixing efficiency parameter is a key measure to determine the height of the flame and its variation with the source velocity is limited by the flame width and the maximum vertical flame velocity at the tip of the flaming region. The variation of different parameters as vertical flame velocity, flame geometry and flame temperature with flame height are shown in plots. It is found that the flame geometry undergoes an initial necking up to a certain height, followed by an increase in its spread thereafter. The flame geometry and the flame dynamics depend exclusively on the burner design and the stack exit velocity. The flame height to burner diameter ratio of the jet diffusion flame is found to vary linearly with Froude number with a constant slope in the logarithmic plot.

**Keywords:** Jet diffusion flame, Necking of flame, Reaction mixing efficiency parameter ( $\phi$ ), Flame height ( $H_f$ ).

---

## 1. INTRODUCTION

A flare system is an essential unit in a petroleum refinery and petrochemical plants. The fuel vapours, while moving upward, entrain air from the surroundings while leaving the tip of the flare stack. The air-fuel mixture is

ignited at an appropriate temperature forming a burning flame. Such a flame is known as the *diffusion flame*. In an alternate arrangement, the fuel is transported in the vapour form through a pipe or burner and is ignited at the tip of the burner. The flame so formed is known as a *jet diffusion flame*. The degree of turbulence along with flame height and flame geometry depends upon the velocity with which the fuel vapours are released. Understanding the flow and thermal dynamics of a *jet diffusion flame* is important for the safety of the plant as well as for a

\* Corresponding author.

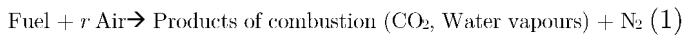
E-mail address: [angan.sengupta@gmail.com](mailto:angan.sengupta@gmail.com); [angan@hyderabad.bits-pilani.ac.in](mailto:angan@hyderabad.bits-pilani.ac.in) (Angan Sengupta).

Peer Review under the responsibility of Universidad Nacional Autónoma de México.

<http://>

number of other scenarios, such as tank leakage or pipeline failure. The intensity of the radiant heat flux from the flame depends on the flame height as well as the height at which the fuel is being released. Hence the determination of the height of a *jet diffusion flame* is important from the view point of the proper operation of flare system and the plant safety.

The diffusion flames may either be turbulent or laminar, depending on the *source Reynolds Number* ( $N_{Re}$ ) (Drysdale, 1985). For  $N_{Re} < 2100$  the flame is considered as a laminar flame, which becomes turbulent as  $N_{Re}$  increases to 4000 or more. Laminar diffusion flame has greater height than a turbulent flame. Because of lateral mixing, the turbulent flames have higher reaction/combustion efficiency; resulting in the consumption of the gas-vapour mixture emanating from the pipe tip at a shorter flame length. The combustion/ reaction in a flame above the pipe tip can be represented as a one-step chemical reaction as follows:



Where,  $r$  is the amount of air required to burn 1 kg of fuel vapour, completely. The rate at which the fuel is consumed is given by (Spalding, 1971):

$$\dot{m}'' = Ap^2 m \left[ m_{O_2} \exp\left(-\frac{E_a}{RT}\right) \right] \quad (2)$$

Where,  $A$  is a dimensionless pre-exponential factor,  $p$  stands for the local pressure (Pa),  $m$  and  $m_{O_2}$  are the local time-mean mass fractions of fuel and oxygen, respectively,  $E_a$  is the activation energy (W),  $R$  the universal gas constant, and  $T$  the time-mean absolute temperature (K). Spalding (1971) suggested the value of  $A$  to be equal to 0.5, and  $E_a/R$  to be 19,000. The turbulent transport phenomena are expressed by the phenomenological Prandtl mixing-length theory. The mixing length is taken as 0.435 times the distance from the wall of the pipe or as 0.13 times the thickness of the local shear layer, whichever is smaller. The reaction efficiency ( $\tau$ ) is defined as

$$\tau = \frac{(m - m_u)}{(m_b - m_u)} \quad (3)$$

The subscripts  $u$  and  $b$  denote the unburnt and fully burnt conditions, respectively. Obviously, the state of a

gas changes from  $\tau = 0$  to  $\tau = 1$  in the course of complete reaction.

The flame length or the flame height (vertical flame) of a jet diffusion flame has been defined in varied ways by various researchers; the axial height from the pipe tip is at which combustion is 99% complete (Hawthorne, Weddell, & Hottel, 1948), the ratio of CO to CO<sub>2</sub> is 0.15 (Hottel, 1961), the fuel mole fraction diminished to 0.0005 (Wade & Gore, 1996). The above definitions are based on the concentration of the fuel and have limitations of the accuracy of the concentration measuring device. Newman and Wiecek (2004) defined the flame length on the basis of the completeness of fuel combustion, relating the yield ratio of CO to CO<sub>2</sub>. For propane, the yield ratio of CO to CO<sub>2</sub> was taken as 0.002. The definition is found to be in agreement with the Heskestad correlation (Heskestad, 1984):

$$H_f / d = -1.02 + 15.6 N^{1/5} \quad (4)$$

Where,  $H_f$  is the flame length (m),  $d$  is the diameter of nozzle (m).  $N$  is a non-dimensional group defined as

$$N = \left[ \frac{c_p T_a}{g \rho_a^2 (\Delta H_c / r)^3} \right] Q^2 / d^5 \quad (5)$$

Where  $Q$  is the heat released from combustion (W) (Heskestad, 1983; Orloff, De Ris, Delichatsios, & Orloff, 1985).  $c_p$  is the specific heat capacity of the reaction mixture (J/kg/K),  $T_a$  is the ambient air temperature (K),  $\rho_a$  is the atmospheric air density at  $T_a$  (kg/m<sup>3</sup>),  $r$  is the stoichiometric air to fuel ratio,  $d$  is the burner nozzle diameter (m) and  $g$  is the acceleration due to gravity (9.81 m/s<sup>2</sup>). For most common fuels,  $\Delta H_c / r = 3100 \text{ kJ/kg}$  (Heskestad, 1999).

Heskestad (1999) defined the flame length as a function of buoyancy momentum parameter ( $R_M$ ),

$$R_M = 0.117 \left[ \frac{\rho_a}{\rho} \right] r^2 N^{2/5} \quad (6)$$

Where,  $\rho$  is the density of the reaction mixture (kg/m<sup>3</sup>). Becker and Liang (1978) correlated the flame height with Richardson number as

$$Ri^{1/3} = \xi_L = \left( \frac{g}{d^2 \left( \frac{\rho}{\rho_a} \right) u_s^2} \right)^{1/3} H_f \quad (7)$$

and a parameter

$$\psi = \frac{d \left( \frac{\rho}{\rho_a} \right)^{0.5} \beta}{H_f \dot{m}} \quad (8)$$

Where,

$$\beta = \left( \frac{M_a T_{ad, st}}{M_{prod} T_a} \right)^{0.5} \quad (9)$$

and  $d$  is the nozzle diameter (m),  $\dot{m}$  is the fuel flow rate (kg/s) and  $u_s$  is the stack exit velocity (m/s). Taking  $\beta = 2.8$  for propane, Becker and Liang (1978) showed that the flame length follows a curve given by,  $\psi = 0.18 + 0.022 \xi_L$  for  $1 < \xi_L < 20$ , provided that the  $N_{Re}$  at the flame tip

was sufficiently high. Kalghatgi (1984) proposed another correlation for the flame length,  $\psi = 0.2 + 0.024 \xi_L$ . Zukoski, Kubota, and Cetegen (1981) conducted a number of experiments on city gas combustion and entrainment in fire plumes and reported the flame heights based on eye measurement with the aid of a meter stick. Correlations for calculating flame length were also given by Thomas (Frank & Lees, 1996) for calm atmosphere conditions as well as for cross-wind conditions. Under calm conditions, the flame height is given by:

$$H_f = 42D \left( \frac{\dot{m}''}{\rho_a \sqrt{gd}} \right)^{0.61} \quad (10)$$

and for cross-wind condition it is given as,

$$H_f = 55D \left( \frac{\dot{m}''}{\rho_a d} \right)^{0.67} (u^*)^{-0.21} \quad (11)$$

Where,  $u^*$  is the dimensionless fuel velocity and is defined as,  $u^* = \frac{u_s}{\left( \frac{g \dot{m}'' d_p}{\rho_v} \right)^{1/3}}$ ,  $\dot{m}''$  is the mass flux of burning

rate of fuel (kg/m<sup>2</sup>/s),  $u_s$  is the stack exit velocity (m/s),  $\rho_v$  is the fuel vapour density (kg/m<sup>3</sup>), and  $d_p$  is the equivalent pool diameter (m). Frank and Lees (1996) has compiled all the available correlations for flame height/length for gas/ gas-vapour mix jet combustion flames.

The flame length depends on the extent of reaction/ combustion as also the wind velocity (accounted for by the air entrainment coefficient), gas-vapour velocity, flame temperature, amount of heat radiated out of the flame and flame geometry. It is also affected by fuel properties such

as fuel composition, the specific heat and the heat of combustion of the fuel. Gas pressure and frequency of flaring in a flare system also determine the height of flames in flare systems. In a flare system, the source velocity is kept 20% - 30% of Mach number ( $Ma = u_s/v_{so}$ ), where,  $v_{so}$  is the velocity of sound (m/s), for desired flame heights, which in turn determines the amount of heat radiated from the flare.

While flame geometry and source velocity/ stack exit velocity ( $u_s$ ) is governed by the burner design, flame temperature is a function of  $u_s$ , wind velocity ( $v$ ) and the burner design (Leahey, Preston, & Stroscher, 2001). For field scale natural gas jet fires, the threshold flame temperature is about 1400 K (Ballie, Caulfield, Cook, & Docherty, 1998). Fairweather, Jones, Lindstedt, and Marquis (1991) used a value of 1200 K for laboratory scale natural gas jet fires. A difference of 200 K in flame temperature will yield a difference of flame length of the order of 20 - 25%. Cumber and Spearpoint (2006) had reported a maximum flame temperature of 1800 K for propane fires by using their probabilistic model. The true flame temperature is less than the adiabatic flame temperature, i.e.  $T < T_{ad}$  and is limited by large

uncertainties. The average radiation temperature also decreases from 1025 °C to 875 °C as wind speeds increased from 1.5 to 3 m/s (Cumber & Spearpoint, 2006). Romero-Jabalquinto, Velasco-Téllez, Zambrano-Robledo, and Bermúdez-Reyes (2016) have presented and described aeronautical use and feasibility of combustion chamber.

In the present paper, an attempt has been made to develop a simplified one-dimensional model to simulate the flame height, flame geometry and temperature. The simulated results for the flame height are also validated with the available experimental data.

## 2. MATHEMATICAL MODEL:

Development of a steady state mathematical model helps in the calculation of the flame height in a stabilized environment. The fire plume formed from a particular fuel is a strong function of the burner design, source velocity and source temperature. The plume once developed, rises due to buoyancy. As the fire plume rises, it entrains air from the surrounding at ambient temperature and thus combustion continues within the reaction zone of the plume. Generally, a fire plume may be divided into two

regions, flaming and non-flaming. The flaming region is near the fire source and all combustion takes place in this region. Above this region is the non-flaming zone where practically no reaction takes place. This is characterized as the thermal plume, which contains the non-reactive products (CO, CO<sub>2</sub> and water vapours) of combustion along with inert nitrogen and a large amount of ambient air. McCaffrey (1979) further subdivided the flaming region as given below:

(a) Accelerating Region:  $0.03 < z/Q^{2/5} < 0.08$  (12)

This is the region of continuous flame and  $u \propto z^{1/2}$  and  $\Delta T$  is constant.

(b) Intermittent Region:  $0.08 < z/Q^{2/5} < 0.2$  (13)

In the intermittent region,  $u$  is constant and  $\Delta T \propto z^{-1}$ .

The mean flame velocity is indistinguishable from the plume velocity in the accelerating region. However, in the intermittent region, sporadic flames are produced, the flame velocity increases until the flame is extinguished, while the mean plume velocity ceases to do so (Gupta, Kumar, & Singh, 1988).

For a flame forming above a cylindrical pipe tip/orifice, the fundamental conservation equations of mass, momentum and energy can be written as (Bird, Stewart, & Lightfoot, 2002):

$$\frac{\partial \rho}{\partial t} + \frac{1}{r_f} \frac{\partial(\rho r_f v)}{\partial r_f} + \frac{\partial(\rho u)}{\partial z} = 0 \tag{14}$$

$$\frac{\partial(\rho u)}{\partial t} + \frac{\partial(\rho u v)}{\partial r_f} + \frac{\partial(\rho u^2)}{\partial z} = g_z(\rho_a - \rho) + \frac{\partial P}{\partial z} \tag{15}$$

$$\frac{\partial(\rho V c_p T)}{\partial t} + \frac{1}{r_f} \frac{\partial(\rho V r_f c_p v T)}{\partial r_f} + \frac{\partial(\rho V c_p u T)}{\partial z} = (-r_A)(-\Delta H_R) V - Q_r A_s \tag{16}$$

Following assumptions can be made for solving the equations of changes under steady state conditions:

- i. Top hat profile governs the radial distribution of temperature and velocity of the flame.
- ii. In the laminar jet diffusion flame air is entrained through the exterior surface of the combustion region and the fuel-air mixture is assumed to be convected upward by the fluid flow within the flame zone (Fay, 2006). The entrainment velocity of the surrounding air ( $v$ ) through the surface of the flame is proportional to the vertical flame velocity ( $u$ ), i.e.  $v = \alpha u$ .

- iii. The physical properties of the reaction mixture (fuel + air) remain constant throughout the flaming zone and the pressure along the radial direction of the flaming zone also remains constant.
- iv. The fuel enters at ambient temperature and pressure.
- v. Heat is lost only by radiation from the flame surface, having an area of  $A_s$ .

Using the above assumptions under steady state condition, and integrating the steady state equations across the radius of the flaming region, the following set of ordinary differential equations are obtained:

$$\frac{d(\rho b u)}{dz} = \alpha u \rho_a \tag{17}$$

$$\frac{d(\rho b u^2)}{dz} = g b (\rho_a - \rho) + b \frac{\partial P}{\partial z} \tag{18}$$

$$\frac{d(\rho b u T c_p)}{dz} = (-r_A)(-\Delta H_R) b - 2Q_r \ln|b| + \rho_a c_p \alpha u (T_a - T) \tag{19}$$

Where,  $b$  is the half plume width and  $Q_r$  is the radiative heat flux. The reaction rate ( $-r_A$ ) could be expressed in terms of the Arrhenius equation to take into account the effect of temperature on the reaction rate. In such a situation, an equation for material balance of fuel can be written and this could be solved by either finite difference method or shooting method. In order to simplify the model, the heat generation term by combustion reaction is expressed as follows (Drysdale, 1985):

$$(-r_A)(-\Delta H_R) = \frac{\dot{m}'' \Delta H_c}{z} = Q_{react} \tag{20}$$

Where,  $\dot{m}''/z$  is the mass burning rate per unit volume (kg/m<sup>3</sup>/s) and  $\Delta H_c$  is the heat of combustion of fuel (J/kg). We also assume that the jet diffusion flame is laminar, which prevents the simultaneous existence of fuel, air and product at the bottom of the combustion zone (Fay, 2006).

The total amount of heat radiated per unit area ( $Q_r$ ) is expressed according to Stefan-Boltzman's relation.

$$Q_r = \epsilon \sigma T^4 \tag{21}$$

Where, the emissivity ( $\epsilon$ ) is equal to 1, for hydrocarbons (Drysdale, 1985).

Equations (17) – (19) and the constitutive relationships, (20) – (21), along with the boundary conditions complete the mathematical description of the jet diffusion flame. The following boundary conditions can be used:

$$\text{At, } z = 0: u = u_s, T = T_s \text{ and } b = b_s \quad (22)$$

The boundary conditions, equation (22), refer to the characteristics of the fire source/ burner at any time ( $t$ ), after the commencement of fire. Initially, it can be assumed that  $T_s = T_a$ , where  $T_a$  is the ambient temperature. The equations (17) – (19) can be written in the following explicit forms:

$$\frac{du}{dz} = \frac{g}{u} \left[ \frac{M_a T}{M T_a} - 1 \right] - \frac{\alpha u}{b} \left[ \frac{M_a T}{M T_a} \right] \quad (23)$$

$$\frac{dT}{dz} = \frac{\alpha M_a T}{b M} \left[ 1 - \frac{T}{T_a} \right] + \frac{\dot{m}'' \Delta H_c R T}{u c_p M P z} - \frac{2 R T \sigma \epsilon T^4 \ln |b|}{P M c_p u b} \quad (24)$$

$$\frac{db}{dz} = \alpha \left[ \frac{M_a T}{M T_a} \right] - b \left[ \frac{g}{u^2} \left\{ \frac{M_a T}{M T_a} - 1 \right\} - \frac{\alpha}{b} \left\{ \frac{M_a T}{M T_a} \right\} \right] - \frac{b}{\rho} \frac{dP}{dz} \quad (25)$$

Equation (24) includes the terms of heat generation by reaction and heat loss by radiation in addition to the entrainment term. Fire is considered as a reaction phenomenon, where the fuel from its liquid or solid state gets converted to its gaseous form prior to the onset of combustion. The density of this gaseous reaction mixture ( $\text{kg}/\text{m}^3$ ) changes with temperature of the fire plume following the ideal gas law:

$$\rho = (PM)/(RT) \quad (26)$$

Where,  $P$  is the ambient pressure (Pa),  $M$  is the molecular weight of the reaction mixture ( $\text{kg}/\text{mol}$ ),  $R$  is the universal gas constant and  $T$  is the flame temperature (K). The subscript ‘ $a$ ’ denotes the air/ ambient condition.

As the fuel gases move upward, air from the surroundings gets entrained according to the equation  $v = \alpha u$ . All the air entrained by the fuel gases does not get mixed with the fuel instantaneously, and a significant mass of entrained air does not participate in the combustion/ reaction. Thus, only a represents of the *mass fraction of the entrained air* ( $\phi$ ) is actually taking part in combustion, on mixing with the fuel, at a particular location of entrainment. This parameter,  $\phi$  is a function of the fuel velocity ( $u$ ). Hence, the mass burning rate of

of the fuel velocity ( $u$ ). Hence, the mass burning rate of the fuel in equation (24) is estimated according to the following relation:

$$\dot{m}'' = \frac{\phi \rho_a \alpha u|_z}{r} \quad (27)$$

Here,  $\phi$  is the reaction mixing efficiency parameter,  $\frac{\rho_a \alpha u|_z}{r}$  gives the mass of air entraining into the flame at an axial distance of  $z$  from the tip of the burner, and  $r$  is the stoichiometric ratio of atmospheric air to fuel. Equation (27) shows that, in reality, the combustion/ reaction inside the flame does not proceed stoichiometrically.

Equations (23) – (25) can be solved numerically by using fourth order Runge–Kutta method, with a step size of 0.01, using the boundary conditions and the equations (26) and (27) for various values of Froude number. The flame height can be defined as the axial distance from the tip of the burner to the top at which the mass flow rate of the reaction mixture becomes zero, i.e.

$$\dot{m}'' \approx 0 \quad (28)$$

This means, the flame height is the axial distance at the end of which the fuel combustion is complete and combustible mixture ceases to exist.

### 3. RESULTS AND DISCUSSIONS:

The developed set of model equations (23) through (25) along with the boundary conditions (equation 22) and equations (26) and (27) has been simulated numerically with the help of fourth order Runge – Kutta method. This method is applicable for both linear and non-linear ordinary differential equations. The method possesses an error of the order of  $\Delta z^5$  per step and an accumulated error of the order of  $\Delta z^4$ , where  $\Delta z$  is the step size. A value of 0.01 is taken as the step size. A source code has been developed in MATLAB, version 7.0.1.24704 to solve the model equations. The processing time required is 15 s. The input parameters of Zukoski, Kubota, and Cetegen (1981) have been used for the solution of the model equations.

Zukoski et al. (1981) had carried out experiments in the laboratory to determine the height of the jet diffusion flame above burners of different sizes. The fuel used in the experiment was a mixture of hydrocarbons.

The fuel contained mainly of methane (0.924 mole fraction), ethane (0.042 mole fraction), nitrogen (0.015 mole fraction) and propane (0.01 mole fraction). The specific heat capacity of the fuel is taken as 2150 J/kg/K, according to its composition. The lower heating value (heat of combustion) of the fuel is taken to be 47.5 MJ/kg and its density is taken to be 0.72 kg/m<sup>3</sup>. The flame produced is assumed to be axisymmetric; and for such a flame, air entrainment coefficient varies from 0.1 to 0.15. The values of the initial source velocity and the burner sizes are given in Table 1.

Physical properties of air, viz. molecular weight of air, and density of air are taken from literature (Perry, Green, & Maloney, 1984). The stoichiometric coefficient is calculated from the fuel parameter (Heskestad, 1999), as described in Section-3, and found to be 15.323. The initial fuel source temperature is taken as 300 K, which is the same as the ambient temperature.

### 3.1 FLAME HEIGHTS:

Table 2 gives a comparison of flame heights as calculated by using the empirical/ semi-theoretical equations proposed by different researchers, for various values of Froude number  $\left(Fr = \frac{u_s}{\sqrt{gb_s}}\right)$ . It is clear that the

values of the flame heights obtained by using different equations differ significantly from one another. Heskestad correlation (Heskestad, 1984) takes into account the buoyancy term in the form of a buoyancy momentum parameter ( $R_M$ ) and also the non-dimensional parameter ( $N$ ). This correlation as proposed by Heskestad, is applicable for pool fires. The Hustad and Sonju model (Frank & Lees, 1996) is valid for methane and propane flames only. The Hustad and Sonju model calculation are based on the parameters of methane. The model proposed by Cook et al. (Frank & Lees, 1996) is a modification of the API model and takes into account the wind effect. MITI model and Considine and Grint model (Frank & Lees, 1996) are mainly used for jet diffusion flames of flashing liquids, and are the best fit for diffusion flames on the surface of an oil storage tank. The Sion - Tan correlation (Tan, 1967) as given by Guigard, Harper, and Kindzierski (2000) is an empirical one.

Table 3 shows the comparison of the values of the calculated flame height by the present model with the experimental data of Zukoski et al. (1981). The predictions

by Cook et al. (Frank & Lees, 1996) and Considine and Grint (Frank & Lees, 1996) are also used for the purpose of comparison. The results of the one dimensional model developed in the present work are in complete agreement with the experimental data of Zukoski et al. (1981). The flame height calculation by the present model assumes that the combustion takes place with some fraction of the entrained air at the elevation of entrainment. From Table 3 one can see that, as the Froude number ( $Fr$ ) increases the flame height also increases for each of the burner type. This is because of poor mixing of fuel and air in the reaction zone. The predictions from this one dimensional model, however, do not take into account effect of wind vector on the radiative heat flux from the flame, which would affect the flame height depending on the prevailing wind velocity, as reported by Sengupta, Gupta, and Mishra (2011) and Da Silva and Landesmann (2014). Both these work employs the point source model (providing larger heat flux) to determine the diffusion pool fire flame height under the various wind conditions. We are in the process of developing more realistic mathematical model that would take the wind velocity effect on the jet diffusion flame height.

Figure 1a illustrates the variation of  $H_f/d$  with  $Fr$ , where  $d$  is the diameter of the burner and is equal to  $2b_s$ . For a given burner diameter increase in  $Fr$  increases the  $H_f/d$  ratio, and hence forming a jet flame. This is because an increase in the source velocity increases the mass flow rate of the fuel, which results in greater flame heights. Moreover, narrower burner produces jet flames of higher  $H_f/d$  ratio for a fixed  $Fr$ . The logarithmic plot between  $H_f/d$  ratio and  $Fr$  (Figure 1b) shows that  $H_f/d$  varies linearly with  $Fr$ , with a slope of 0.6 (hydrocarbon mixture flame (Thomas, 1962) for all burner diameters.

An increment in source velocity amplifies the  $H_f/d$  ratio, as shown in Figure 2. A jet flame with greater  $H_f/d$  ratio is found to have a higher value of  $Q^*$  (Figure 2), where

$$Q^* = \frac{\dot{m}\Delta H_c}{d^{\frac{5}{2}}c_p T_a \rho_a \sqrt{g}} \quad (29)$$

Zárate, Lara, Cordero, and Kozanoglu (2014) have also reported of an initial increase in the total heat flux with an increase in the flame height of a jet flame.

### 3.2 FLAME TEMPERATURE AND REACTION MIXING EFFICIENCY PARAMETER:

Figure 3, gives the axial temperature profile within the flame, for different  $Fr$ . With an increase in  $Fr$ , the height of attaining the maximum flame temperature ( $T_{max}$ ) also increases. This is because of the fact that the mass burning rate increases with an increase in the stack exit velocity. A decrease in reaction mixing efficiency parameter ( $\phi$ ) at  $Fr = 3.566$  and  $0.891$  (Figure 3a) further increases this height for attainment of  $T_{max}$ . It has been observed that, the temperature of the flame increases initially because of combustion; as it is an exothermic process. The total heat loss due to radiation is not significant at this stage. In the later stage as the flame rises upwards, the heat loss due to radiation increases as the flame temperature rises. Because of the radiation loss, the flame temperature starts decreasing particularly along the flame height at the end of the combustion zone. Secondly, in the combustion zone; fuel combustion generates heat energy that causes an increase in temperature of the reaction mixture close to the adiabatic flame temperature as the radiant heat loss is less significant in this part of the flaming region. At the upper edge of the combustion region, however, most of the fuel has been consumed and there is no further increase in the thermal energy, though an increase in the momentum flux in this region (refer Figure 8a) increases the air entrainment, which along with predominant radiant heat loss cools the reaction mixture. This phenomenon results in the formation of a peak in the temperature distribution, as shown in Figure 3a. A similar trend of the temperature profile was also observed by Cumber and Spearpoint (2006) from their mathematical model of propane jet flame. Wang, Li, Mei, and Mi (2013) also noted similar temperature profile along the flame height, for different volume fraction of oxygen taking part in the combustion.

From the experiment of Zukoski et al. (1981) and also from the present model (illustrated in Figure 3a), it is observed that, for the burner with  $b_s = 0.05$  m; an initial increase of source velocity ( $u_s$ ) from  $0.588$  m/s to  $2.355$  m/s (75% increase) results in a 33% increase in flame height ( $H_f$ ). Further increase in source velocity, for the same burner, by only 33% increases  $H_f$  by 35%. Similarly, for the burner with  $b_s = 0.1$  m; an initial increase in  $u_s$  by 52%, followed by an increase of 31% increases the flame height by 33% and 35%, respectively. While the initial 33% increase in  $H_f$  is because of the enhancement in mass

flow rate of the fuel alone, the increase of  $H_f$  by 35% later, with a relatively small increment in  $u_s$  (as against of 75% and 52%, respectively) is due to the combined effect of the increase in the mass flow rate of the fuel and a decrease in the reaction mixing efficiency parameter ( $\phi$ ). The reduction in the mixing time of the fuel with air with an increase in the  $Fr$  to 3.566 and 0.891, for the burners with diameters of 0.1 m and 0.2 m, cause a decrease in the value of  $\phi$  (Figure 4a) and hence reduces the  $T_{max}$  by 6.5% and 11% (Figure 3a), respectively. For the burner diameter of 0.5 m we also observe an initial increase in the value of  $\phi$  followed by a decrease with an increase in the  $Fr$  (Figure 4a). Thus, for all the experimentally generated flames as reported in the literature from each of the three burner designs (Zukoski et al. 1981); the present model shows a decrease in the value of  $\phi$  following an increase in its value with an increase in the  $Fr$  (Figure 4a). However, for a given amount of mixing between the fuel and the entrained air;  $T_{max}$  increases with an increase in  $Fr$  for a given burner dimension (Figure 3b). This is because of the increase in the mass burning rate of the fuel with an increase in  $u_s$ . The reduction in the value of  $\phi$  with an increase in the flare stack exit velocity is found to follow the following inequality, for all the cases studied by the present model:

$$\theta_{max} = \frac{b_{max}}{u_{max}} > 0.1s \quad (30)$$

Where,  $b_{max}$  is the maximum half plume width attained by the jet flame and  $u_{max}$  is the maximum velocity of the fuel at the top of the flaming region. Thus,  $\theta_{max}$  in some way gives the measure of the time required by the flame to attain its fully developed geometry. Figure 4b shows the variation of reaction mixing efficiency parameter ( $\phi$ ) with  $\theta_{max}$  for burners with diameter 0.1m, 0.2 m and 0.5 m and we observe that the reaction mixing efficiency parameter decreases for all values of  $\theta_{max} > 0.1$ .

Figure 5a shows the variation of  $T_{max}$  with source velocity,  $u_s$ . For a given value of  $\phi$ , an increase in the flow rate of the fuel from the burner of fixed diameter increases the mass burning rate and hence the maximum temperature of the flame. Similarly, the  $T_{max}$  is found to be greater for a flame with greater flame height ( $H_f$ ) and with fixed reaction mixing efficiency parameter of 40%, as shown in Figure 5b. Similar trends of  $T_{max}$  with  $u_s$  and  $H_f$  were reported by Cumber and Spearpoint (2006).

Moreover, it is noted from Figures 5a and 5b that a decrease in burner diameter reduces the maximum flame temperature and enhances the flame height. Thus, it can be concluded that, as the flame become more jet-like

(greater  $H_f/d$  ratio) with  $b_s$  decreasing; the maximum flame temperature decreases, while the maximum flame temperature increases with increasing flame height due to an increase in stack exit velocity.

Table 1. Input Parameters (Zukoski et al.1981).

Burner Diameter (m)	Initial Source Velocity (m/s)	Air Entrainment Coefficient ( $\alpha$ )
0.1	0.588	0.11
0.1	2.355	0.11
0.1	3.532	0.11
0.2	0.416	0.11
0.2	0.866	0.11
0.2	1.248	0.11

Table 2. Comparison of the Calculated Values of Flame Height from Different Models.

$b_s$	$Fr$	Calculated Values of Flame Height (m) Using the Equations of					
		Heskestad (1984)	Hustad & Sonju	Cook et. al.	MITI Model	Considine & Grint	Sion-Tan (1967)
0.05	0.594	1.995	1.773	0.996	1.889	0.525	12
0.05	2.377	3.55	2.339	1.932	3.29	1.05	12
0.05	3.566	4.193	2.537	2.346	3.869	1.286	12
0.1	0.297	2.975	3.087	1.637	2.863	0.883	24
0.1	0.618	4.057	3.574	2.325	3.839	1.274	24
0.1	0.891	4.729	3.845	2.768	4.444	1.529	24

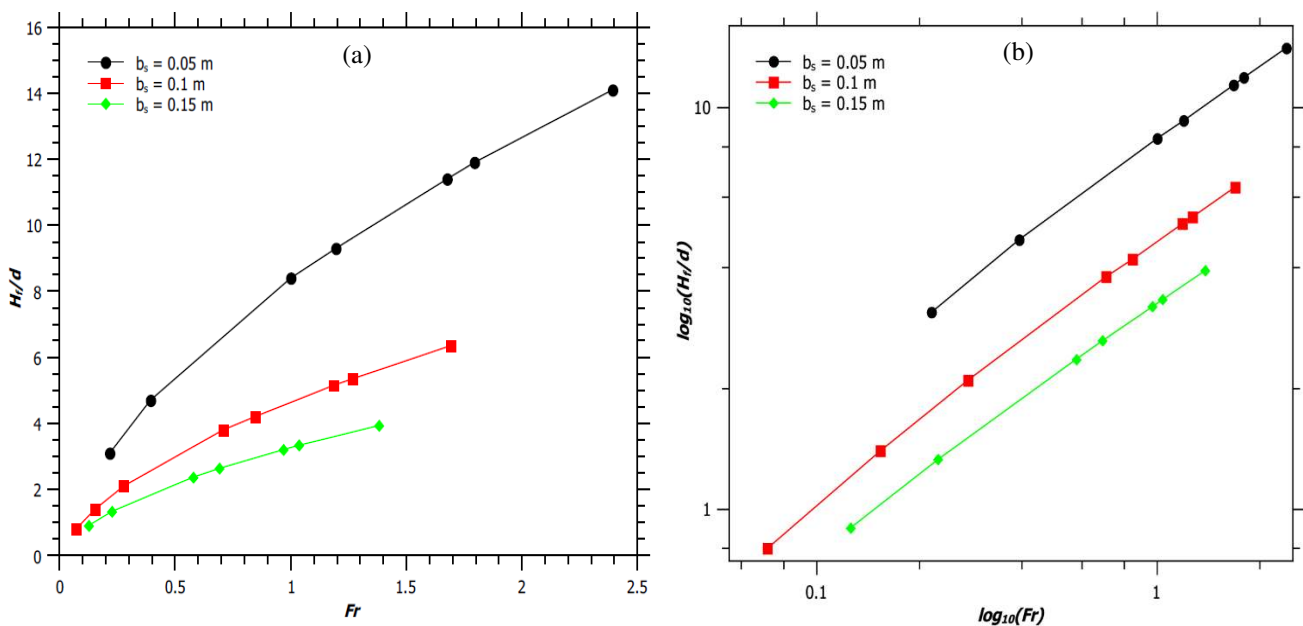


Fig. 1. (a) Variation of  $H_f/d$  ratio with Froude number. (b) Logarithmic plot of  $H_f/d$  ratio with Froude number.



Table 3. Comparison of Estimated Flame Heights (m) with Zukoski et al. (1981), Experimental Data, and other Jet Flame Models.

$b_s$	$Fr$	Zukoski et al. (1981), (Expt. data)	Cook et al.	Considine & Grint	Present Model	Deviation (%)	
						Cook et al.	Considine & Grint
0.05	0.594	1	0.996	0.525	1	0.4	47.5
0.05	2.377	1.5	1.932	1.05	1.5	-28.8	30.0
0.05	3.566	2.3	2.346	1.286	2.3	-2.0	44.1
0.1	0.297	1	1.637	0.883	1	-63.7	11.7
0.1	0.618	1.5	2.325	1.274	1.5	-55.0	15.1
0.1	0.891	2.3	2.768	1.529	2.3	-20.4	33.5

Note: Deviation (%) =  $\frac{\text{value from present model} - \text{value of other model}}{\text{value from present model}} \times 100$

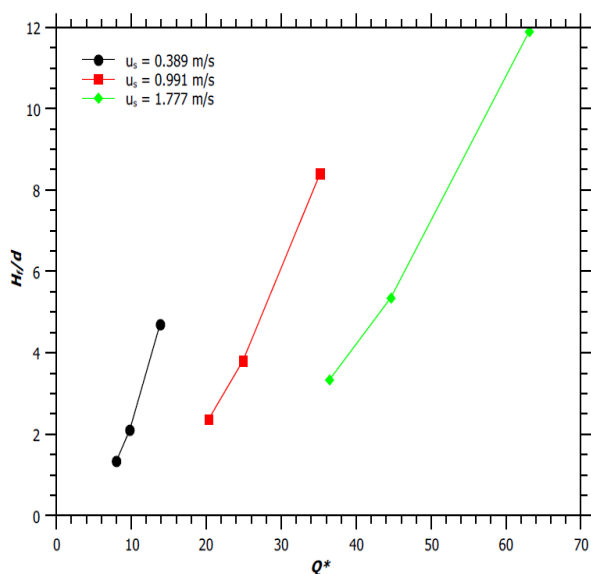


Fig. 2. Variation of  $H_f/d$  ratio with  $Q^*$ .

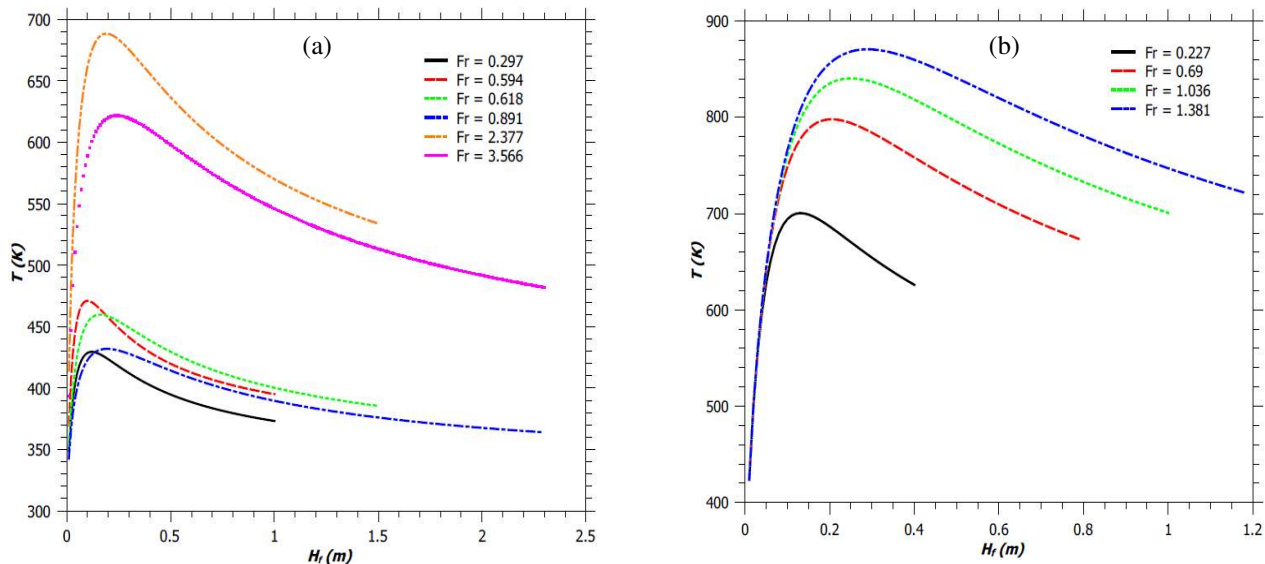


Fig. 3. Axial flame temperature of a jet flame. (a) Flames described by Zukoski et al. (1981). (b) Simulated flames.

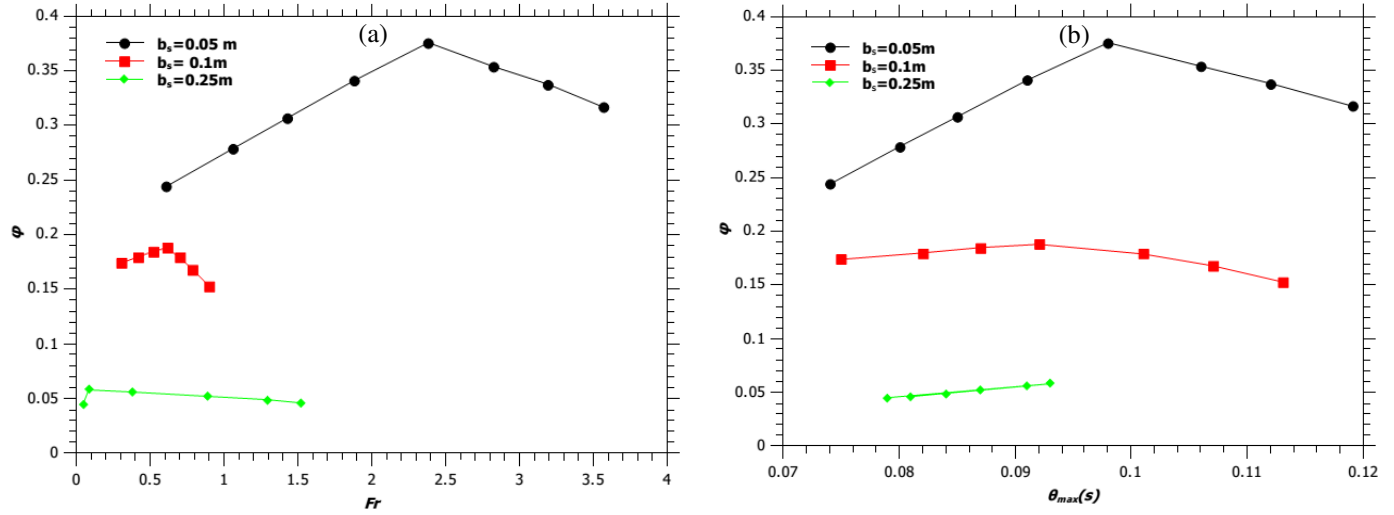


Fig. 4. (a) Variation of reaction mixing efficiency parameter ( $\phi$ ) with Froude number. (b) Variation of reaction mixing efficiency parameter ( $\phi$ ) with  $\theta_{max}$ . Solid lines are guide way to eyes.

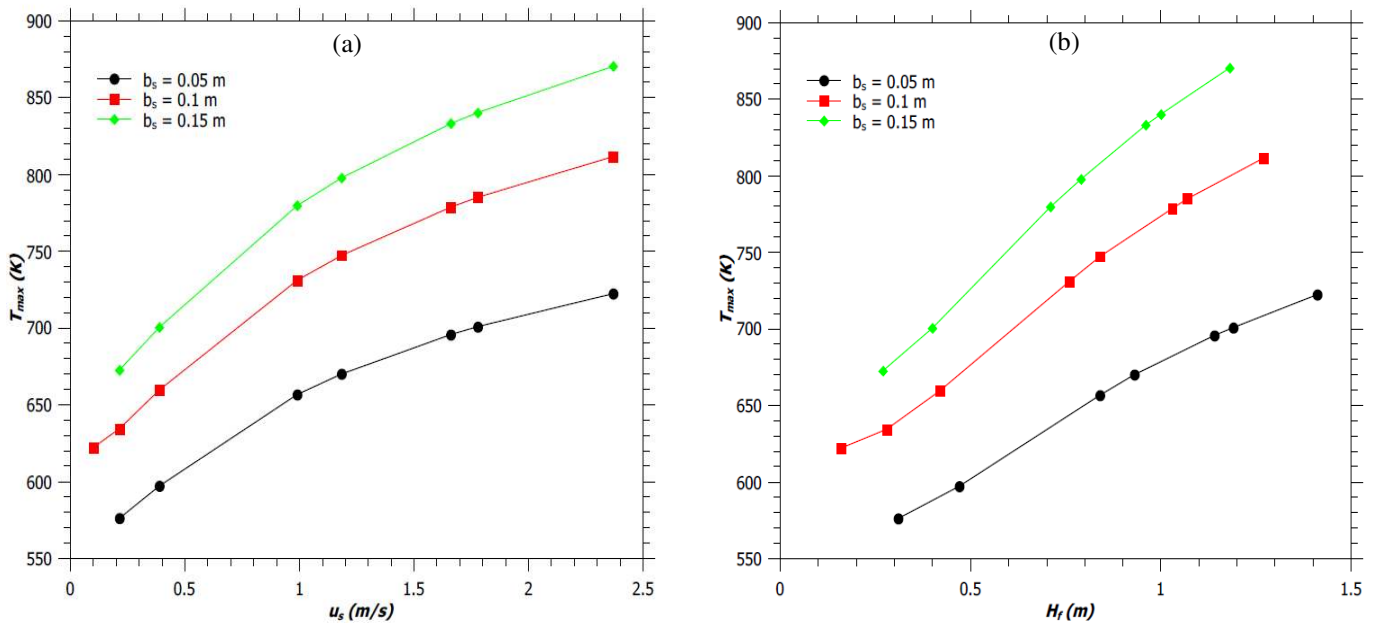


Fig. 5. (a) Variation of maximum flame temperature ( $T_{max}$ ) with source velocity ( $u_s$ ). (b) Variation of maximum flame temperature ( $T_{max}$ ) with flame height ( $H_f$ ). Solid lines are guide way to eyes.

### 3.3. FLAME GEOMETRY AND VELOCITY:

The velocity profile within the flame and the flame geometry has been obtained using the present model for the flames described by Zukoski et al. (1981). Figure 6 shows the flame geometry for various  $Fr$  values. The flame geometries for jet diffusion flames as reported by Zukoski

et al. (1981) and for jet diffusion flames with fixed reaction mixing efficiency and for fixed burner design have been illustrated in Figure 6a and Figure 6b, respectively. For  $Fr < 1.0$ , the flame width initially decreases along the flame height. This phenomenon is known as the ‘necking of the flame’. At this point, the half width of the plume is minimum,  $b_{min}$ .

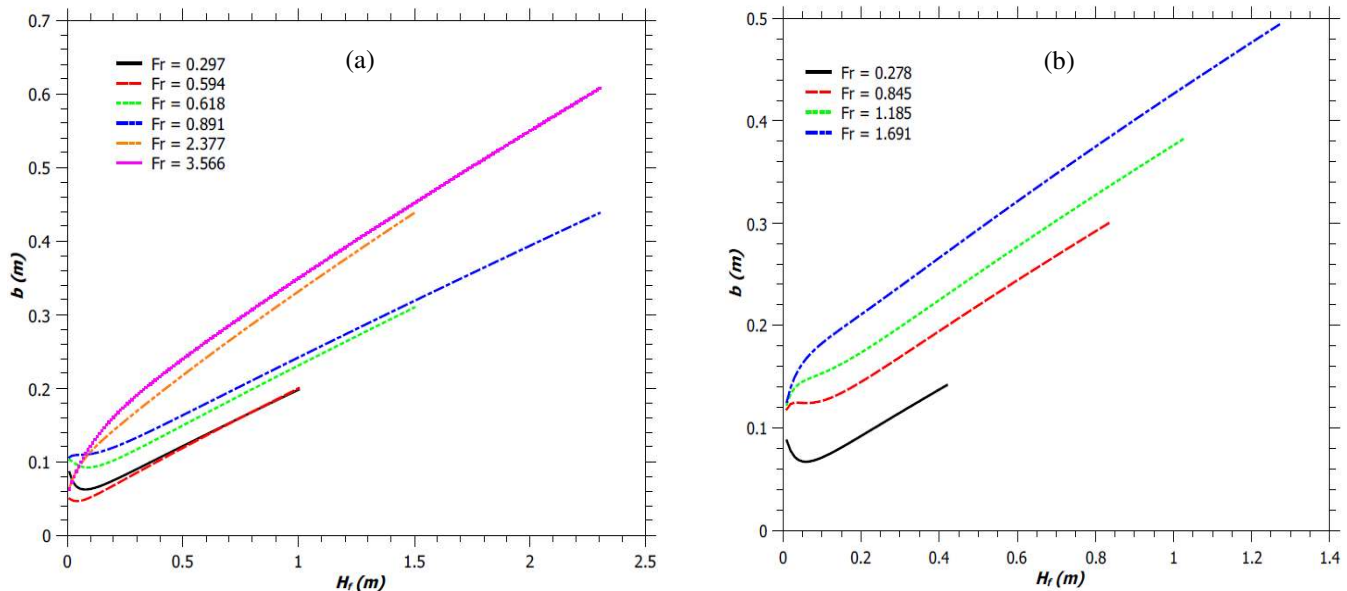


Fig. 6. Radius of the flaming zone in a jet flame. (a) Flames described by Zukoski et al. (1981). (b) Simulated flames.

Thereafter,  $b$  starts increasing and the flame assumes the shape as described by Gupta (1990) and also by the Carven model (Frank & Lees, 1996). The  $b_{min}$  is about 0.046 – 0.092 m for all the low values of  $Fr$ . Figure 7 shows the variation of the maximum radius,  $b_{max}$ , of the flaming zone with Froude number. It's seen that for any given  $b_s$ , the  $b_{max}$  increases with an increase in  $Fr$ . Similarly, for any  $Fr$  value,  $b_{max}$  increases with an increase in  $b_s$ . As the fuel-air mixture rises, the vertical jet velocity increases as shown in Figure 8. This results in an increase in the entrainment of air into the plume according to the equation,  $v = \alpha u$ , as discussed earlier. The increasing air entrainment increases the volume of the reaction mixture and results in an increase of the flame width (Figure 7). Moreover, for a fixed  $Fr$ , burner with narrower diameter produces flame of smaller width, as shown in Figure 7. Hence jet flame with higher  $H_f/d$  ratio, have smaller flame width, as expected (by comparing Figures 1a and 7).

The variations of the axial flame velocity for jet diffusion flames as reported by Zukoski et al. (1981) and for jet diffusion flames with fixed reaction mixing efficiency and for fixed burner design have been illustrated in Figure 8a and Figure 8b, respectively. From Figure 8, we can observe that the vertical flame velocity increases until the flame gets extinguished. This was reported by McCaffrey (1979) too. For  $Fr < 2.0$ , the vertical flame velocity increases monotonically with the flame height. This result in more entrainment of air and hence an increase in the flame width. For  $Fr > 2.0$ , there is an initial

decrease of flame velocity followed by its monotonic increase along the flame height. An increase in  $Fr$  increases the maximum flame velocity, due to enhanced inertia and buoyant force. However, for a fixed  $Fr$ , a burner with a narrower diameter produces a flame with lower vertical flame velocity, as shown in Figure 9. Thus, jet flame with higher  $H_f/d$  ratio, has lower maximum vertical flame velocity at the tip of the flaming region, as expected (by comparing Figures 1a and 9).

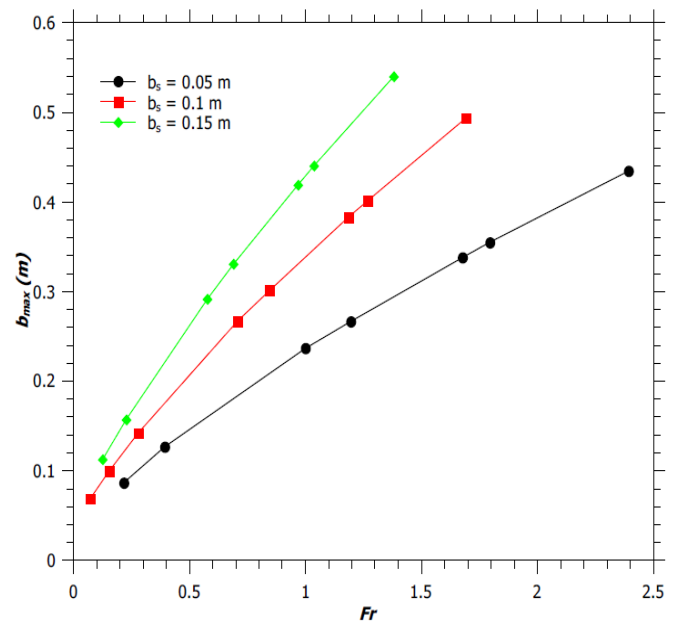


Fig. 7. Variation of the maximum radius of the flaming zone in a jet flame with Froude number.

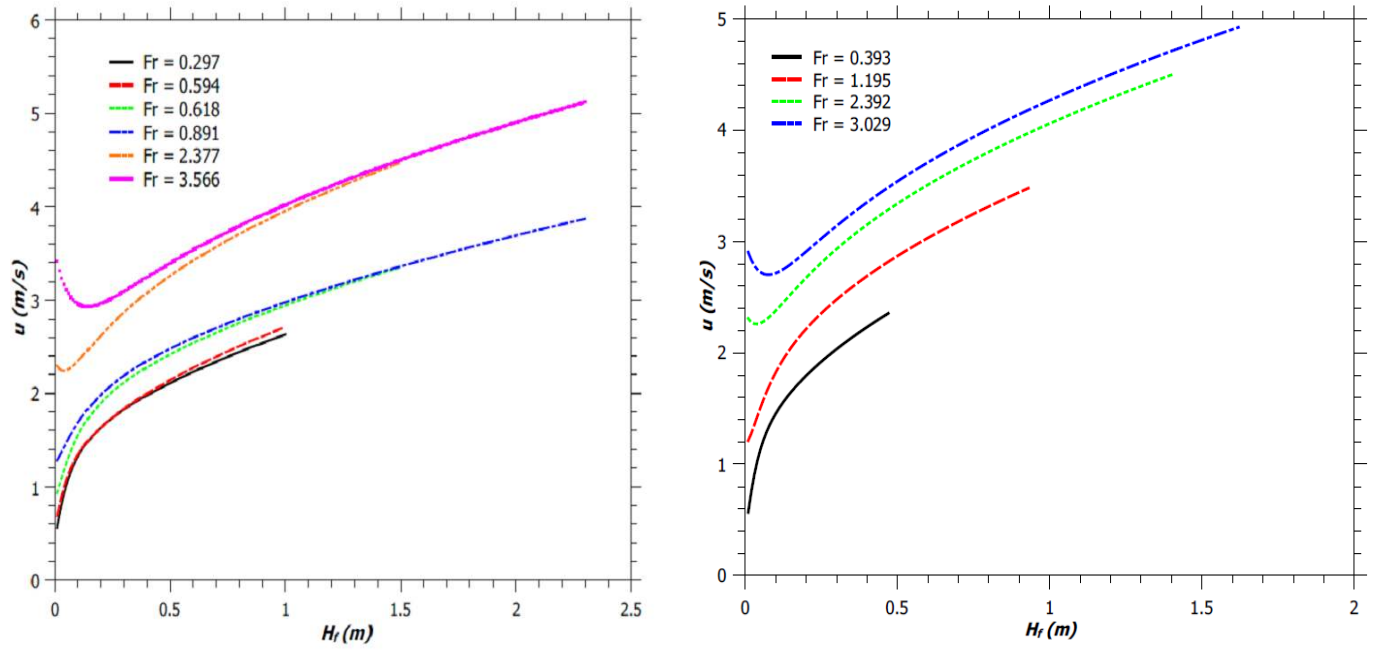


Fig. 8. Vertical jet flame velocity. (a) Flames described by Zukoski et al. (1981). (b) Simulated flames.

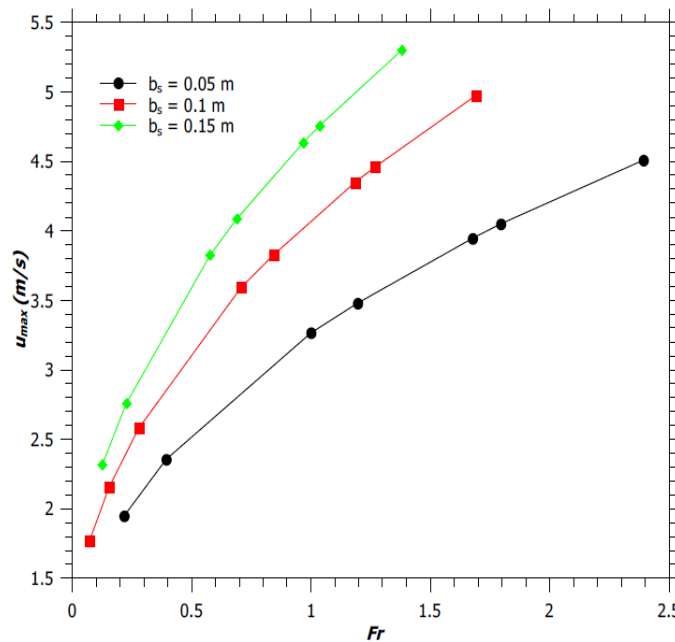


Fig. 9. Variation of maximum vertical flame velocity with Froude number.

#### 4. CONCLUSION:

The one dimensional jet diffusion flame model in a flare system can be used to predict the behavior of the flare – the axial temperature profile, the flame geometry, and its velocity variation along the flame length. The developed one-dimensional model provides correct

estimate of the experimentally determined flame height under no wind conditions, though we obtain a narrower peak in the temperature distribution along the flame height as compared to the data reported in literature (Cumber & Spearpoint, 2006). The flame height to burner diameter ( $H_f/d$ ) ratio, as predicted by the model, is found to approach a value of jet-like flames with an increase in

the stack exit velocity and with a decrease in the burner diameter. However, the logarithmic variation of this ratio with the Froude number is linear having a constant slope of 0.6.

Due to an increase in temperature within the flame, vertical flame velocity increases because of increased buoyancy until the end of the flaming region of the plume. The plume rises mainly due to the buoyant force. A minimum initial fuel source velocity is required for the jet flame to form. The total quantity of the fuel is not combusted with the amount of immediately entrained air. This phenomenon is illustrated with a reaction mixing efficiency parameter ( $\phi$ ). The fraction of the fuel-air mixture reacting in the flame depends on the reaction time available for the fuel-air mixture. The fraction of air thus taking part in the reaction is determined by the value of  $\phi$ . It is observed that,  $\phi$ , initially increases with an increase in stack exit velocity ( $u_s$ ); because of more entrainment of air; and thereafter decreases as the reaction time available decreases with an increase in  $u_s$ . The increase in the value of  $\phi$  is limited by the value of  $\theta_{max}$ , which is to be less than 0.1 s to maintain the increase in the reaction mixing efficiency parameter with the change in  $u_s$ .

The width of the jet flame produced by a flare system increases after an initial necking over a short flame length, for  $Fr < 1.0$ . The necking of the flame decreases with an increase in stack exit velocity. The height of the flame mainly depends on the initial mass flow rate of the fuel and also on the extent of combustion of fuel-air mixture, taking place in each grid. While the heat generation is by the combustion/ reaction, the heat loss takes place mainly due to radiation. As a consequence of the process of combustion and radiation occurring simultaneously, a jet diffusion flame which is formed with higher  $H_f/d$  ratio has smaller flame width and lower maximum vertical flame velocity at the tip of the flame.

The prediction of the flame geometry by the present one dimensional jet diffusion flame model corresponds to the flame geometry predicted by Gupta (1990) and by the Carven model (Frank & Lees, 1996). The predicted flame height of the jet diffusion flame is in good agreement with the experimentally observed flame height, given by Zukoski et al. (1981). However, it is clearly seen that the flame height as calculated from the various models available in literature give results that varies widely as compared to the experimentally observed flame height.

## ACKNOWLEDGEMENTS

One of the authors<sup>a</sup> wishes to acknowledge the financial support, in form of fellowship, received from Indian Institute of Technology, Roorkee for carrying out the research work. The authors also acknowledges the use of facilities of IIT Roorkee and BITS-Pilani for the above work.

## CONFLICT OF INTEREST

The authors have no conflicts of interest to declare.

## REFERENCES

- Baillie, S., Caulfield, M., Cook, D. K., & Docherty, P. (1998). A phenomenological model for predicting the thermal loading to a cylindrical vessel impacted by high pressure natural gas jet fires. *Process safety and environmental protection*, 76(1), 3-13. doi.org/10.1205/095758298529209
- Becker, H. A., & Liang, D. (1978). Visible length of vertical free turbulent diffusion flames. *Combustion and Flame*, 32, 115-137. doi.org/10.1016/0010-2180(78)90087-1
- Bird, R. B., Stewart, W. E., & Lightfoot, E. N. (2002). *Transport phenomena*. 2nd. New York.
- Cumber, P. S., & Spearpoint, M. (2006). A computational flame length methodology for propane jet fires. *Fire safety journal*, 41(3), 215-228. doi.org/10.1016/j.firesaf.2006.01.003
- Da Silva Santos, F., & Landesmann, A. (2014). Thermal performance-based analysis of minimum safe distances between fuel storage tanks exposed to fire. *Fire Safety Journal*, 69, 57-68. doi.org/10.1016/j.firesaf.2014.08.010
- Drysdale, D. (1985). *An introduction to fire dynamics*. John Wiley & Sons.
- Fairweather, M., Jones, W. P., Lindstedt, R. P., & Marquis, A. J. (1991). Predictions of a turbulent reacting jet in a cross-flow. *Combustion and Flame*, 84(3-4), 361-375. doi.org/10.1016/0010-2180(91)90012-Z
- Fay, J. A. (2006). Model of large pool fires. *Journal of hazardous materials*, 136(2), 219-232. doi.org/10.1016/j.jhazmat.2005.11.095
- Frank, P. L., & LEES, F. (1996). *Loss prevention in the process industries*. Butterworth-Heinemann, 15(1).
- Gupta, A. K., Kumar, S., & Singh, B. (1988). One-dimensional mathematical modelling of enclosure fire dynamics. *Fire and materials*, 12(2), 51-60. doi.org/10.1002/fam.810120203
- Gupta, A. K. (1990). *Studies on mathematical modeling of fire dynamics* (Doctoral dissertation, PhD Thesis, Department of Chemical Engineering, IIT, Roorkee).

- Guigard, S., Harper, N., & Kindziarski, W. B. (2000). Heat radiation from flares. Science and Technology Branch, Environmental Sciences Division, Alberta Environment.
- Hawthorne, W. R., Weddell, D. S., & Hottel, H. C. (1948). Mixing and combustion in turbulent gas jets. In *Symposium on Combustion and Flame, and Explosion Phenomena* 3(1), 266-288). Elsevier.
- Heskestad, G. (1983). Luminous heights of turbulent diffusion flames. *Fire safety journal*, 5(2), 103-108. doi.org/10.1016/0379-7112(83)90002-4
- Heskestad, G. (1984). Engineering relations for fire plumes. *Fire Safety Journal*, 7(1), 25-32. doi.org/10.1016/03797112(84)90005-5
- Heskestad, G. (1999). Turbulent jet diffusion flames: consolidation of flame height data. *Combustion and Flame*, 118 (1-2), 5160. doi.org/10.1016/S00102180(98)00161-8
- Hottel, H. C. (1961). Fire modeling. In *International Symposium on the Use of Models in Fire Research*. National Academy of Sciences, National Research Council Washington, DC.
- Kalghatgi, G. T. (1984). Blow-out stability of gaseous jet diffusion flames. Part I: in still air. *Combustion Science and Technology*, 26(5-6), 233-239. doi.org/10.1080/00102208108946964
- Leahey, D. M., Preston, K., & Strosher, M. (2001). Theoretical and observational assessments of flare efficiencies. *Journal of the Air & Waste Management Association*, 51(12), 1610-1616. doi.org/10.1080/10473289.2001.10464390
- McCaffrey, B. J. (1979). Report NBSIR 79-1910. National Bureau of Standards.
- Newman, J. S., & Wiecek, C. J. (2004). Chemical flame heights. *Fire safety journal*, 39(5), 375-382. doi.org/10.1016/j.firesaf.2004.02.003
- Orloff, L., De Ris, J., Delichatsios, M. A., & Orloff, L. (1985). Chemical modeling of gaseous species in turbulent fires. Factory Mutual Research.
- Perry, R. H., Green, D. W., & Maloney, J. O. (1984). *Perry's Chemical Engineer's Handbook* Chemical Engineer's Handbook. McGraw-Hill.
- Romero-Jabalquinto, A., Velasco-Téllez, A., Zambrano-Robledo, P., & Bermúdez-Reyes, B. (2016). Feasibility of manufacturing combustion chambers for aeronautical use in Mexico. *Journal of applied research and technology*, 14(3), 167-172. dx.doi.org/10.1016/j.jart.2016.05.003
- Sengupta, A., Gupta, A. K., & Mishra, I. M. (2011). Engineering layout of fuel tanks in a tank farm. *Journal of Loss Prevention in the Process Industries*, 24(5), 568-574. doi.org/10.1016/j.jlp.2010.06.016
- Spalding, D. B. (1971, January). Mixing and chemical reaction in steady confined turbulent flames. In *Symposium (International) on Combustion*, 13(1), 649-657). Elsevier. doi.org/10.1016/S0082-0784(71)80067-X
- Thomas, P. H. (1962). The size of flames from natural fires. *Fire Safety Science*, 497, 1-1.
- Tan, S. H. (1967). Flare system design simplified. *Hydrocarbon Processing*, 46(1), 172.
- Wade, R. W., & Gore, J. P. (1996). Visible and chemical flame lengths of acetylene/air jet diffusion. In 1996, NISTR 5904: 41-42. NIST Annual Conference on Fire Research.
- Wang, F., Li, P., Mei, Z., & Mi, J. (2013). Auto-and forced-ignition temperatures of diffusion flames obtained through the steady RANS modeling. *Energy & Fuels*, 28(1), 666-677. Doi: 10.1021/ef4022416
- Zukoski, E. E., Kubota, T., & Cetegen, B. (1981). Entrainment in fire plumes. *Fire safety journal*, 3(3), 107-121. doi.org/10.1016/0379-7112(81)90037-0
- Zárate, L. G., Lara, H. E., Cordero, M. E., & Kozanoglu, B. (2014). Infrared thermography and CFD analysis of hydrocarbon jet fires. *Chem Eng Trans*, 39, 1357-1362.